

CHOPPING FREQUENCY OPTIMIZING IN THE NIR MOISTURE METER

Mirko Filic, Venco Corluka and Zdravko Valter

Moisture meter, NIR, near infrared, chopping frequency

1. Introduction

The moisture measuring is realised via reflected radiation at specific wavelengths in near infrared region (NIR). Because it has been noted that NIR although being inappropriate for the qualitative spectrometry, can at the same time be very acceptable for the quantitative analytics of some individual substance kinds including water [2]. The substance containing it has a great impact on that kind of moisture measuring and it makes the measuring to be more complex.

The optoelectronic part of the NIR moisture meter designed and realised by the authors is analysed in this paper. The infrared radiation measurement system is based on the cooled PbS photoconductive detector and a mechanical chopper. The signal obtained from the detector is very small and mixes with the noises from various sources. However, the basic function of the proposed measuring system is to separate the useful signal from the overall signal, to amplify it to the level which can be acquired and post processed by the matching PC digital system. Partially it is effectuated by the mechanical chopper which in conjunction with a detector converts the NIR beam to the alternating photocurrent. Its frequency can be chosen by the rotary speed of the chopper control with the electric drive. In addition, the noise reduction and increasing signal to noise ratio are realised by the AC coupled analogue preamplifier with the power line noise filter. The optimum frequency and rotary speed of the chopper drive are at the same time disposed by the theoretical analysis and with the experiments on the proposed measuring system.

2. Conditioning PbS detector signal in the infrared moisture meter

The NIR radiation is produced by the halogen lamp. The narrow band of reference beam at 1800nm and of the absorbed beam at 1940nm are selected by the optic filters [2] and directed to the sample. The rotational wheel of the mechanical chopper has nine symmetric distributed circular sockets and is situated between lamps and sample. So the selected beam, the reference at the first and the absorbed at the second time are chopped with the rotational wheel and the alternating reflected radiation falls into the photodetector.

2.1 Electronic part of the measuring system

The characteristics of PbS photoconductive detectors such as high detection levels in wavelengths of between 1000nm and 3200nm, good response speed and reasonable price, mean that they can be used in various applications for the moisture detection due to one distinctive absorption wavelength of water at 1940nm [2]. Thanks to the radiation chopping and the use of alternating signal, the response time is limited by the chopping frequency. The block diagram of the proposed measuring system is shown in Fig.1. The bias voltage for the supply detector and the other active elements for the conditioning signal are obtained by the stabilized rectifier supply module from the AC power line. The small AC signal from the detector is conditioned by the AC

coupled analogue pre-processing circuit. The preamplifier that is embodied by several functionally different stages and the frequency filter for additional elimination of the power line generated noise of 50Hz from the useful signal are separately labelled in Fig. 1.

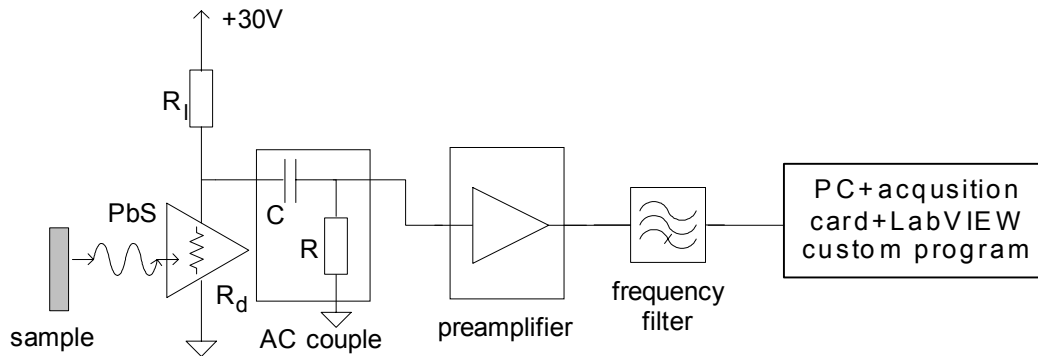


Figure 1. Block diagram of the electronic part of the measuring system

2.2 Basic noise sources in the measuring system

Different noise sources are observed in the proposed measuring system so the corresponding noises are denoted as the detector noises, the background (photon) noise, the noises generated by the power source and the noises of signal processing circuit.

The equivalent model [6] of the noises generated in the detector and in the power source with the supply module is shown in Fig. 2. The measuring signal is represented by the signal current generator (I_{ph}). Its level gets in the levels of the noises when the measuring system works normally.

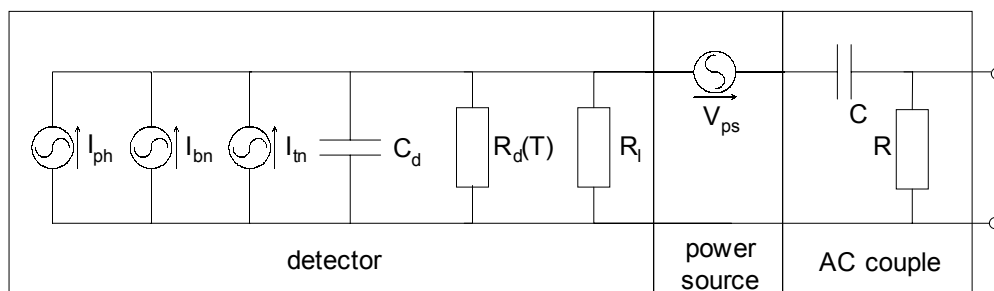


Figure 2. Noise model of the detector and power source

Therefore, the dominant noise sources are the detector, the background and power source, but the noises are generated by the operational amplifiers with JFET and by other elements of the signal processing circuit which are here neglected. The detector noises appear due to the thermal excited carriers in the detector at the actual temperature value which has over 0K, so they are represented by the thermal generated noise (I_{tn}) in Fig. 2. The dark resistance value, depending on the temperature inside the detector element ($R_d(T)$), diversifies the fluctuation of the measured signal together with its relative resistance variation, its temperature coefficient and bandwidth needed in the measuring system. It is together with its relative resistance variation, its temperature coefficient and bandwidth needed in the measuring system diversifying the fluctuation of the measured signal. The detector has a significant thermal generated noise at the working temperature due to its high dark resistance value. The reduction of the thermal excited carriers as well as the decreasing of the detector noise can be ensured by the cooling detector. The noise and thermal drift characteristics of the detector vary from one end to the other of the same type, which characterise the internal processes that govern the operation of the detector. Due to the great disparity between the values of the detector parameter with respect to the typical item, the particular calibration data by the manufacturer are provided. C_d and R_l are the equivalent capacity of the detector and the load

resistance, respectively. The background generated noise (I_{bn}) can not be estimated exactly. It depends on various parameters like the case material, the surface ruggedness and the colour, the absolute temperature, the type (PbS) and active area of the applied detector and the chopping frequency. Whole metal surfaces of the moisture meter are blacked by the blackening material for its high and near uniform absorption. The blackening material is chosen to provide the incident background radiation to the detector area to be as minimal as possible. For example, the peak radiated energy depends on absolute temperature of the environment and varies when it is changing. The background noise can be reduced by narrowing the detector's field of view. Furthermore, the incident background radiation flux which enters vertically to the detector area can be achieved by designing appropriate moisture meter construction. This noise can be weighty in the case of a very low signal and very low detector noises, but due to the discrete nature of radiation, which is composed of photons arriving randomly in time, this noise can be generated by actual desired signal photons. Absorbed photons composed either in the background flux or in the desired signal flux produce photoelectrons at random intervals, and its variation in current appears as noise. When that occurs, the detector system operates in a background limited performance mode (BLIP).

All active elements are supplied from AC power source by rectifier module. The infrared source, the drive of filter wheel and thermoelectrical cooler in the detector are supplied from the same power supply module, too. Consequently this module comprises six different rail voltage-current levels. Although the separate outputs from the power supply module are stabilized, the harmonic noise is produced by either the AC power source or by the supply module (V_{ps}). Odd multiples of the power line frequencies are usually expressed. These noises have the same level as is the voltage signal from the detector and therefore have been filtered by the frequency filter. Further noise filtering is executed by the choice of the mechanical chopper frequency. This is accomplished by means of the rotary speed of filter drive adjustment. The signals versus noise characteristics of the detector as well as the impact of the power line generated noise to the operating circuit require a choice of higher frequency. In addition one common practice is applied, removing power line generated noise from the system so that the chopping is adjusted at an odd multiple of $\frac{1}{2}$ the line frequency of the power source.

2.3 Frequency response of the pre-processing circuits

The input impedance of the preamplifier circuit due to used operational amplifiers with JFET is high and its impact on the total detector load is neglected. Total detector load (Fig.2) is frequency depended and can be expressed by

$$Z_1(j\omega) = R_1 \frac{1 + j\omega CR}{1 + j\omega C(R + R_1)} \quad (1)$$

where ω is the rotary frequency which is corresponding to the chopping frequency. The magnitude versus frequency characteristics can be shown at the normal working area by

$$|Z_1(\omega)| = R_1 \frac{R}{R + R_1} \quad (2)$$

but the maximum useful signal value from the detector is obtained when the detector load is equal to the dark resistance of the detector.

The transfer function of the AC couple is

$$G_{RC}(s) = \frac{sT_1}{sT_1 + 1} \quad (3)$$

where the time constant is $T_1=RC$.

Similarly the preamplifier shown in Fig. 1 can be specified by the following transfer function

$$G_p(s) = K \frac{\omega_1^2}{s^2 + s2d_1\omega_1 + \omega_1^2} \frac{s^2}{s^2 + s2d_2\omega_2 + \omega_2^2} \quad (4)$$

where K is the gain of the preamplifier, ω_1 and d_1 are the undamped natural frequency and the damping ratio of the low pass analogue filter respectively and ω_2 and d_2 are the undamped natural frequency and the damping ratio of the high pass analogue filter respectively. The frequency filter from Fig. 1 is represented by the transfer function

$$G_f(s) = \frac{s^2 + \omega_3^2}{s^2 + s2d_3\omega_3 + \omega_3^2} \quad (5)$$

where the ω_3 and d_3 are the undamped natural frequency and the damping ratio of the band limited analogue filter respectively. The frequency characteristic of the AC coupled preamplifier with the frequency filter with parameters $K=3759$, $T_1=47\text{ms}$, $\omega_1=6190.4\text{s}^{-1}$, $\omega_2=644.7\text{s}^{-1}$, $\omega_3=312.9\text{s}^{-1}$ and $d_1=d_2=d_3=1$ is shown in Fig. 3.

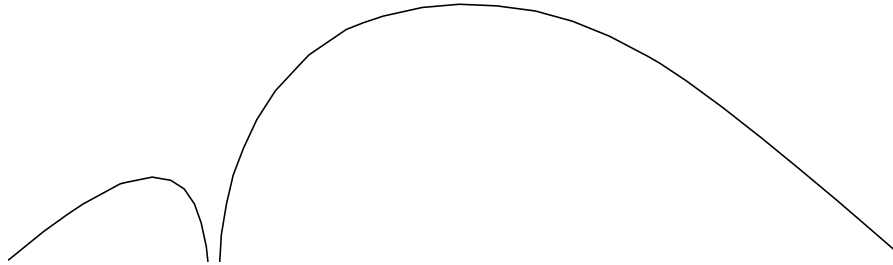


Figure 3. Frequency characteristic of the preamplifier with frequency filter

The mentioned parameters are chosen to provide the maximum value of the amplification in the frequency range which contains the optimal chopping frequency as presupposed. The cutoff frequencies 156Hz and 854Hz are marked in Fig. 3.

3. Examples and measuring results

Many of the output signals from the preamplifier are measured at the constant temperature of the photodetector and ambient 22°C for the same wheat grain sample with known moisture content of 16% at various chopping frequencies up to 800Hz. Time response and frequency response of these output signals at the rotary speed of the chopper 4225.2min^{-1} (70.42Hz) are shown in Fig. 4.

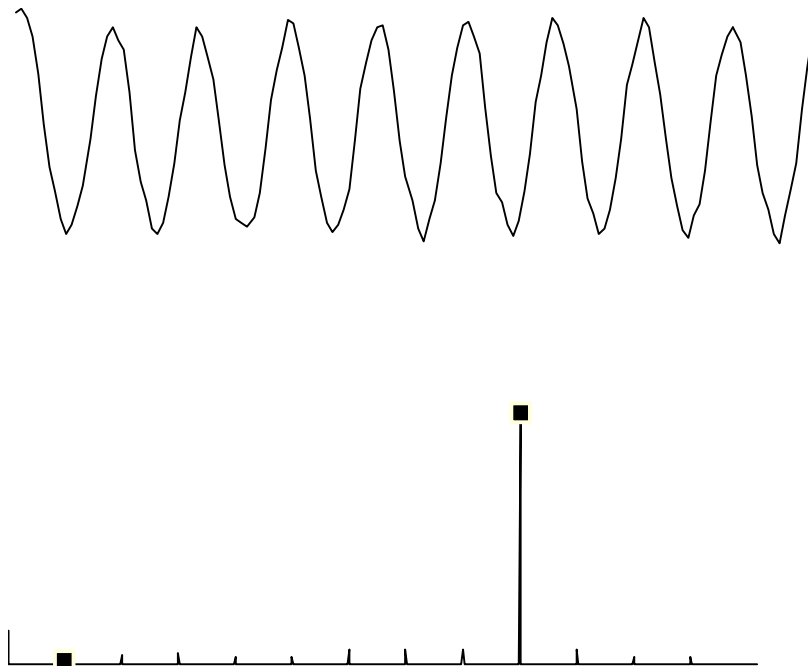


Figure 4. Time response a) and frequency response b)

The expressed frequency response is calculated by the discrete Fourier transformation from the time response. Since there are nine holes in the chopper wheel, the basic chopping frequency of the reflected beam is defined as the 9th harmonic of the rotary speed frequency. It is 633.8Hz for the marked speed 4225.2min⁻¹, Fig. 4b). The high order frequency components as well as the basic frequency of the rotary speed except the chopping frequency exist in the output signal due to the applied frame of the optical filter windows. The frequency content can be changed by the appropriate frame or/and size of the hols chosen in the filter wheel. All measured output signals over the frequencies from 316Hz to 800Hz are shown by the curve in Fig. 5c). This frequency range is extracted from Fig. 3 and the amplification of the analogue pre-processing circuit is shown in Fig. 5b). The output signals from the detector are given by the computation of the output signal versus amplification ratio and are shown in Fig. 5a).

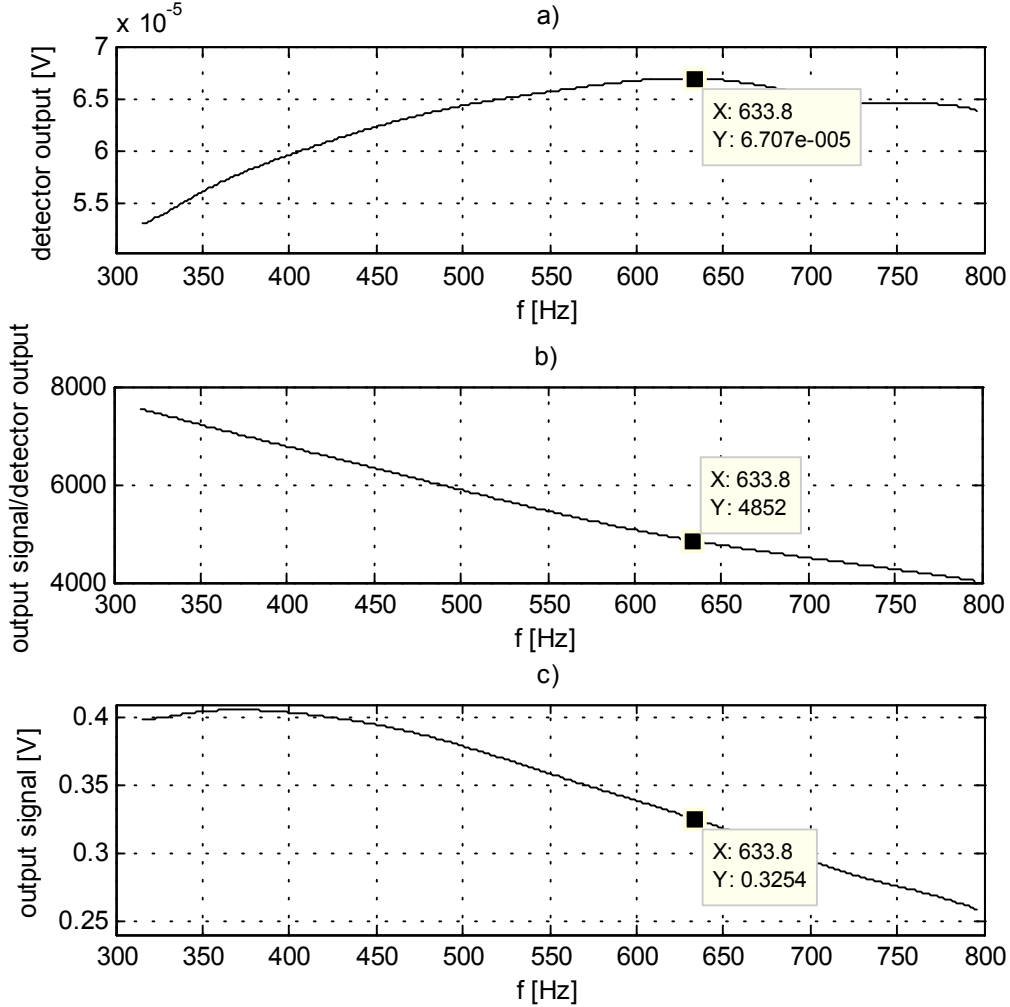


Figure 5. Output signal from detector a), amplification b) and output signal of the pre-processing circuit c)

The output signals from detector increase when the chopping frequency increases to the marked 633.8Hz. It can be explained by the decreasing characteristics of the total noise values in the output signal from detector when the chopping frequency is increasing. Furthermore, the ulterior enlargement of the chopping frequency results in the decreasing of output signals from detector so the frequency responses of the useful voltage signal from the detector are given as

$$V(f) = \frac{V_0}{\sqrt{1 + (2\pi f\tau)^2}} \quad (6)$$

where V_0 is DC response [V] and τ is time constant [μ s]. The time constant τ depends on the detector temperature and it increases when the detector is cooled.

4. Conclusions

The measuring system of the NIR moisture meter based on the cooled PbS photoconductive detector is developed by the authors. The theoretical and practical analyses in this paper are based on the measuring results considering the different chopping frequencies at the same environment and detector element temperatures. The detector temperature is measured by the embedded thermistor. At 633.8Hz, the maximal output signal from detector is obtained and it was found out that it is the optimal chopping frequency in which the value of the signal to noise ratio is maximal at the given temperature. The frequency response of this measuring system is measured and computed from the time response by the discrete Fourier transformation. However, the detector characterises the internal processes that govern its operation and the values of the parameters vary from typical items just as they vary when the temperature of the detector element is changed. It can result for some other chopping frequencies to be optimal. It has not been investigated yet, but it can be the topic of our next research. The noises which are produced by other elements in the analogue pre-processing circuit like the operational amplifier and its impact on the measuring system have not studied yet. It is supposed that they are small in comparison to the detector noises, background noises and power source generated noises across all the ranges of useful frequencies and they do not have influence on the current measuring results.

Many problems can be anticipated when the signal of the reflected beam is small and its level fails into the levels of the total detector noises. It can be partly solved by increasing the total detector load as the reserve is remarked by (1) and partly by increasing the detectivity via the decreasing of the temperature with the thermoelectrical cooler which is embedded in the detector. The output signal from detector can be increased by increasing the total density the incident radiation which is captured, but it all needs further investigation.

References

- [1] Corluka, V.; Filic, M.; Mesic, M. & Valter, Z. (2004). Near infrared based moisture meter, Proceedings Elmar-2004, Kos, T. & Grgic, M. (Ed.), pp. 412-417, 1334-2630, Zadar, June 2004, Croatian Society Electronics in Marine-ELMAR, Zadar
- [2] Corluka, V.; Filic, M.; Mesic, M. & Valter, Z. (2004). Optoelectronic moisture measurement, Proceedings of the 3rd DAAAM International Conference on Advanced Technologies for Developing Countries, Katalinic, B., Veza, I. & Bilic, B. (Ed.), pp. 303-308, ISBN 953-6114-68-2, Split, June 2004, Univ. of Split, Faculty of Electrical Engineering, Mechanical Engineering and Naval Architecture, Split
- [3] Corluka, V.; Filic, M. & Valter, Z. (2004). Development of one infrared moisture meter, Proceedings of the 15th DAAAM International Symposium "Intelligent Manufacturing & Automation", Katalinic, B., Wien, November 2004, DAAAM International Vienna, Wien
- [4] Mesic, M.; Filic, M. & Valter, Z. (2005). Experience with Detectors for Infrared Moisture Measuring, *Proceedings of 6th Int. Conf. on "Electromagnetic Wave Interaction with Water and Moist Substances"*, Kupfer, K. (Ed.), pp. 535-540, Weimar, June 2005, MFPA, Weimar
- [5] Günzler, H. & Gremlich, H.-U. (2003), *IR-Spektroskopie*, Wiley-VCH Verlag GmbH & Co. KGaA, ISBN 3-527-30801-6, Weinheim
- [6] Bielecki, Z.; Kolosowski, W.; Dufrene, R. & Borejko, M. (2003), Low noise optical receivers, Proceedings of 11th GAAS Symposium, pp. 137-140, Munich, 2003, Munich
- [7] Geladi P. & Dabbak E. (1995) An overview of chemometrics applications in near infrared spectrometry, *Journal of Near Infrared Spectroscopy*, 3(3), 1995, 119-132

MSc.Mirko Filic,

Faculty of Electrical Engineering, J.J.Strossmayer University of Osijek, Department for Power and Electric Machinery, Trpimirova 2b, 31000 Osijek, Croatia, tel.031 224 630, fax. 031 224 605, moby: 098 391 615, E-mail: Mirko.Filic@etfos.hr

Venco Corluka, dip.ing.

Faculty of Electrical Engineering, J.J.Strossmayer University of Osijek, Department for Electric measuring, Trpimirova 2b, 31000 Osijek, Croatia, tel.031 224 600, fax. 031 224 605, E-mail: Venco.Corluka@etfos.hr

PhD, full professor Zdravko Valter,

Faculty of Electrical Engineering, J.J.Strossmayer University of Osijek, Department for Power and Electric Machinery, Trpimirova 2b, 31000 Osijek, Croatia, tel.031 224 631, fax. 031 224 605, E-mail: ZValter@etfos.hr